Magnetic Characterization of SMCs

Author: Jesús Urtasun Elizari
Facultat de Física, Universitat de Barcelona, Diagonal 645, 08028 Barcelona, Spain.

Advisors: Dr. Javier Tejada Palacios[1] & Dr. Arturo Lousa Rodriguez[2]
[1] *Departamento de Física Fundamental y Consituyentes de la Materia, Facultat de Física, Universitat de Barcelona. and*
[2] *Departamento de Física Aplicada y Óptica, Facultat de Física, Universitat de Barcelona.*

Abstract: In this article we will discuss the nature of Soft Magnetic Composites (SMCs) magnetization, with special emphasis on deep understanding of magnetic losess and their sources. SMCs are usually characterized by having high saturated magnetization, and extremely low coercivity fields. Measuring the complex magnetic permeability, we will try to describe the behavior in the Hz, MHz frequency range. This document focuses in the deep understanding of one particular composite and its complete characterization. Hysteresis cycle obtained by SQUID measurements and laser diffraction, to determine the mean size and distribution of particles, are exposed.

I. INTRODUCTION

SMCs are ferromagnetic materials which present an extremely thin hysteresis cycle, and have high magnetic permeability, so they experience a huge magnetic induction when they are submitted to en external field [1]. They are involved in a lot applications, as processing electronic signals and suppressing electromagnetic interferences (EMI). Fe, Si and common ferrites are examples of those kind of materials, together with metallic alloys and the composites shown here.

SMCs studied through this article present a periodic structure composed by iron core particles, compacted from powder to form a soft magnetic bulk [2]. To have zero electrical conductivity, those particles are wrapped in an isolating coating, composed by an inorganic compound. Through this article we try to discuss the nature of these particles and their covering, in order to understand the origin of their magnetic properties in the Hz, MHz frequency range. As we will show, we observe both an extremely low coercivity field and a huge saturation magnetization with barely no sources of dispersion, when we submit it to an external magnetic field above 1T.

We will work with different SMCs tagged as AHD, H118, H121, H123 and 700IP, together with iron particles named H31. Laser diffraction measurements obtained in the *Unidad de Citometría* of the *Parc Cientific de Barcelona* allowed us to determine the mean size of particles, which we try to relate to the magnetization and permeability behavior.

As we see in figure 1, SMC H118 presents a gaussian size distribution, with the mean size of particles in 200 μm, meanwhile all the rest of SMCs and the iron particles have the same distribution with the normal value on 100 μm. Laser diffraction measurements also allowed us to verify the reliability of the screened samples prepared of the different SMCs shifts, which we discuss later.

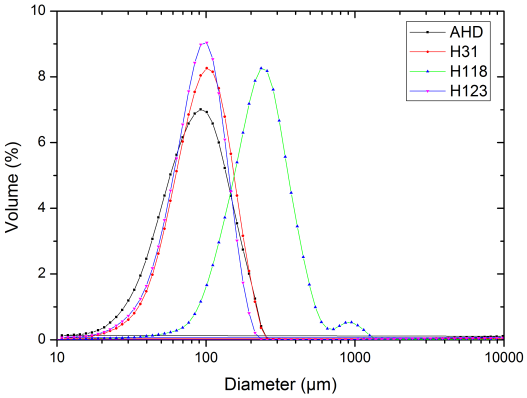

FIG. 1: Percentage of particles vs the particle diameter, for the different SMCs and iron particles (H31).

Measuring the complex magnetic permeability and analyzing direct measurements of magnetization using a Superconductor Quantum Interference Device (SQUID), we try to relate its behavior to the mean size of particles, and the single domain particle behavior.

II. THEORETICAL MODEL

A. Magnetic domains. Exchange & anisotropy

First of all, we describe our system as a bulk ferromagnet, conformed by an homogeneous distribution of magnetic domains, and domain walls isolating every individual state of spin, of size λ [3]. The spins of a magnetic solid are arranged in order to minimize their exchange energy, given by the Heisenberg model

$$H_{ex} = -\frac{1}{2} J \sum_{i \neq j} \boldsymbol{s}_i \boldsymbol{s}_j \tag{1}$$

For an exchange constant $J > 0$, the order that minimizes the energy is a ferromagnetic one, and for $J < 0$ we obtain an anti-ferromagnetic order. Once the lattice has chosen an order, the direction of the total magnetization will be given by the anisotropy of the material. We can now write the expression for the size of the domain walls in terms of the exchange energy and the magnetic anisotropy as

$$\lambda = a\sqrt{\frac{E_{ex}}{E_A}} \tag{2}$$

Notice that as the anisotropy of the material increases, the domain walls become thinner, and it's easier to reverse the magnetization.

We observe that magnetic materials use to invest the total magnetization when they are submitted to an external field, instead of changing the estate of particular spins. This is because investing only one, or a few of magnetic momenta implies overcoming the exchange energy. Investing the total magnetization preserves the order and only implies overcoming the anisotropy, which is typically much lower.

B. Magnetic permeability

Magnetize a system means carrying it to a metastable state of energy, so the magnetization always experiences a relaxation process with time that can be described by the differential equation

$$\tau \frac{dM}{dt} + M = 0 \tag{3}$$

When we submit it to an alternating field of the form $H(t) = H_0 cos(\omega t)$, the magnetization follows the field as

$$M(t) = \chi H_0 cos(\omega t) \tag{4}$$

If we add now the effect of the relaxation due to the domain wall movement, the equation (2) becomes non-homogeneous

$$\tau \frac{dM}{dt} + M = \chi H cos(\omega t) \tag{5}$$

and the magnetization follows the law

$$M(t) = \chi(\omega) H_0 cos(\omega t) \tag{6}$$

being $\chi(\omega)$ the complex magnetic susceptibility. The components χ_1 and χ_2 will be the coefficients of the real and the imaginary part, respectively in phase and with a phase shift from the applied field, and they are given by

$$\begin{aligned} \chi_1 &= \frac{\chi}{1 + (\omega\tau)^2} \\ \chi_2 &= \frac{\chi\omega\tau}{1 + (\omega\tau)^2} \end{aligned} \tag{7}$$

In the next section we compute the complex permeability $\mu_r = \mu/\mu_0 = (\chi + 1)$ by measuring the impedance of toroidal shifts.

III. EXPERIMENTAL

We will first analyze the direct measurements of magnetization obtained by the SQUID magnetometer. The SQUID uses superconductor currents to induce a magnetic field, preserving the analyzed shift in liquid Helium to measure at extremely low temperatures. To measure the hysteresis cycle $M(H)$, we had to prepare extremely light shifts, of 0,5 mg - 1 mg. Above that weight, the magnetization of SMCs was so high that it saturated the measurement table, and it could not be recorded. Experimental results are shown in the next section.

We focus now on the sources of dispersion . To measure them, we need to measure the complex impedance $Z(\omega)$ of toroidal shifts prepared with the different powder SMCs, together with iron particles to compare their behavior at high frequency. These measurements were done using an impedance analyzer HP 4192A between 5 Hz -13 MHz. The system measures the in-phase and in-quadrature components of the current. Due to the high instability obtained at low frequencies, we show the 1KHz - 13MHz range. As mentioned before, we measure the modulus or "effective" permeability $\mu = \mu_0(1 + \chi)$ involved in the law

$$B = \mu_0(H + M) = \mu_0(1 + \chi)H = \mu_0\mu_r H \tag{8}$$

so its behavior is the same as the susceptibility derived in section II, when we applied an alternating field. The measured permeability can now be written as

$$\mu(\omega) = \mu'(\omega) - i\mu''(\omega) \tag{9}$$

being $\mu(\omega)$ the complex magnetic permeability. Our equivalent circuit is a RLC containing the inductance L of the coil, the resistance R of the copper wire and a small capacity effect. Representation of our experimental equipment is shown below.

The relation between the measured impedance Z and the parameters R and L of the sample is given by [5]

$$R + i\omega L = Z' + iZ'' \tag{10}$$

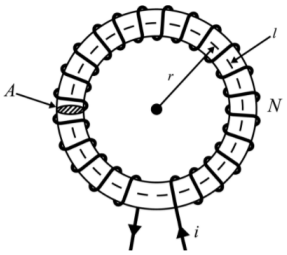

FIG. 2: Representation of the experimental equipment, corresponding to an equivalent circuit RLC [4].

Now the components of the permeability μ' and μ'' can be obtained directly from the complex impedance [5]

$$\mu'(\omega) = \frac{L^{'}(\omega)}{L_0} = \frac{Z^{''}(\omega)}{\omega L_0}$$
$$\mu''(\omega) = \frac{L^{''}(\omega)}{L_0} = \frac{Z^{'}(\omega)}{\omega L_0} \quad (11)$$

being ω the frequency of the applied field, and L_0 the inductance of the toroid without the ferrite inside

$$L_0 = \frac{\mu_0 N^2 d}{2\pi} ln(\frac{b}{a}) \quad (12)$$

IV. RESULTS & DISCUSSION

A. Magnetization

We observe that SMCs present a very similar magnetization than iron particles, having the typical ferromagnetic behavior mentioned in section I. We measured the magnetization from 0 to 16000 Oe, and back to zero field. As expected, SMCs present barely no remanent magnetization, which implies that there are no energy losses, and there is almost free to invest the magnetization, being the coercivity field $H_c \simeq 0$.

As we see in figure 3, different SMCs (H118, H123, 700IP) differ only in 0,05 - 0,1 emu with iron particles, when we compute the magnetization normalized per unit of mass.

Notice that the magnetization does not saturate for small applied fields. It needs about 1 T to achieve the saturation value. This behavior contrasts with other soft magnetic composites as FeSi alloys, which use to saturate very quickly, presenting both a thin hysteresis, and a very pronounced increase at low fields.

Laser diffraction measurements also allowed us to verify the reliability of screened samples obtained from the Geology faculty. By measuring these samples, doing Zero Field Cooled - Field Cooled (ZFC - FC) measurements [6], we can estimate the blocking temperature, which remains $T_B > 300K$ for an applied field $H = 5000$ Oe.

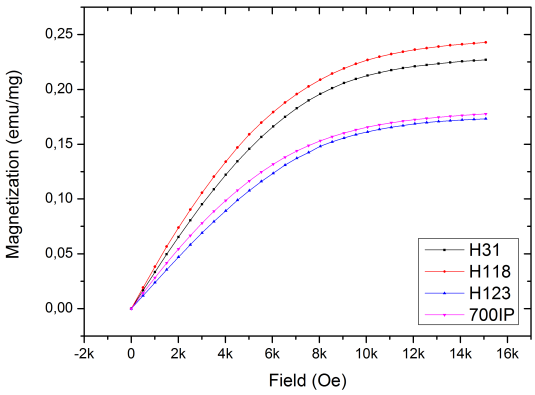

FIG. 3: Magnetization normalized per unit mass of iron particles (H31) and different samples of SMCs.

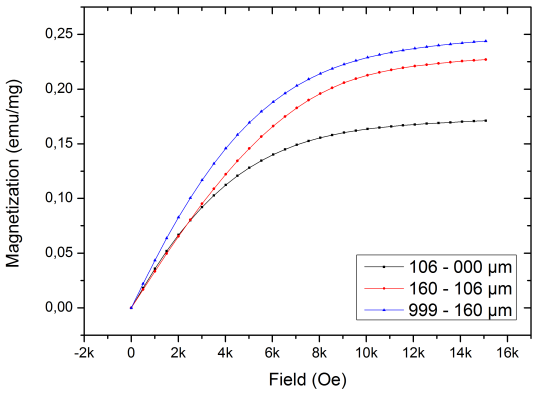

FIG. 4: Magnetization of screened samples H31. The biggest particles are the ones that achieve a the maximum value of the saturation magnetization.

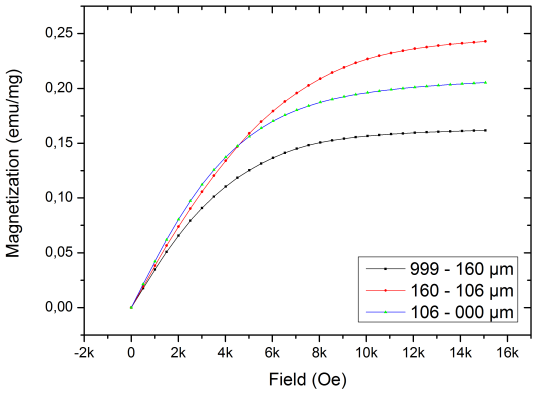

FIG. 5: Magnetization of the screened samples H118.

B. Permeability

We observe in figure 6 the behavior of the complex permeability, being 100 KHz the frequency for which the material experiments a decay of the "effective" permeability. At this frequency there is an absorption of the energy from the external field, as we see in the peak of the component μ''. We say that there is a resonance effect at this point, as the frequency of the applied field matches with the frequency of the spin rotation. For higher frequencies, the modulus of the permeability decays as the real part, and the material does not feel the magnetic field. As mentioned before, due to this absorption phenomenon SMCs are used to suppress and screen electromagnetic interferences.

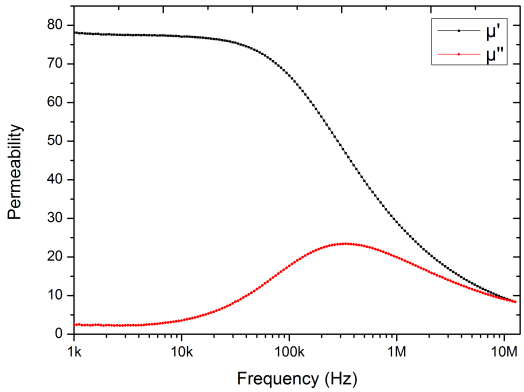

FIG. 6: Components of the permeability vs frequency of the applied field for SMCs H118. We observe both, the decay and the absorption peak of the real and the imaginary components of the permeability.

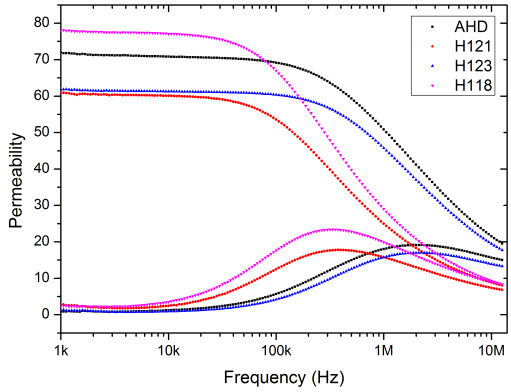

FIG. 7: Comparison of the components of the permeability vs frequency of the applied field. The absorption peak varies smoothly between the different SMCs toroidal samples.

The size distribution $f(V)$ implies a different behavior of μ', μ''. As we narrow the sizes distribution, both the real and imaginary components of the permeability become more pronounced. For an ideal system composed by particles of a unique size, μ' will decay as a Heaviside function, and μ'' will become a Kronecker's delta at the value of the frequency for which we observe the absorption. This behavior can be observed in the figure 8, that shows the permeability of the different screened samples for one particular SMC.

Here we expose the computation of the susceptibility, integrated now for a bulk of volume V.

$$\chi_1 = \chi_0 \int_0^\infty dV \frac{f(V)V}{1+(\omega\tau)^2}$$
$$\chi_1 = \chi_0 \int_0^\infty dV \frac{f(V)V\omega\tau}{1+(\omega\tau)^2} \tag{13}$$

being $\int_0^\infty dV V f(V) = N\langle V\rangle$. If we introduce the blocking volume

$$V_B = \frac{K_B T}{K} ln(\frac{\nu}{\omega}) \tag{14}$$

at low temperatures the factor $(1+(\omega\tau)^2)^{-1}$ becomes the Heaviside function $\theta(V - V_B)$.

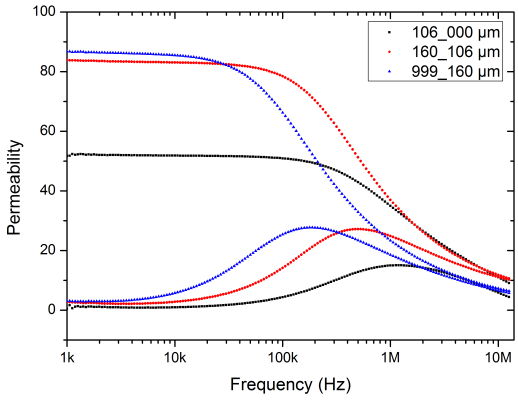

FIG. 8: Components of the permeability vs frequency of the applied field for different screened samples of SMCs - 700IP. We observe the different behavior of μ' μ''. The smallest particles present the absorption peak displaced to the right, which means that the absorption takes place at higher frequencies.

We can verify the dependence with $f(V)$. Until 160 μm the material presents different size particles, having an homogeneous distribution, and the components μ' μ'' present respectively a soft decay, and a weak absorption peak. But the more pronounced decays of the component μ' show that most of the particles have a mean size of 160 μm and 999 μm.

Notice that this behavior contrasts with the one observed in the previous section, as the extremely thin hysteresis is typical of much smaller particles, that can behave as single domain particles.

C. Infrared Spectroscopy

We should now focus on the covering that isolates the iron core particles, which gives them zero electrical conductivity, and may be the responsible of structural properties such as the huge ductility and malleability.

As other phenomenon that may involve the covering, we have the slow increment of the magnetization until it achieves the saturation value, shown in figure 2.

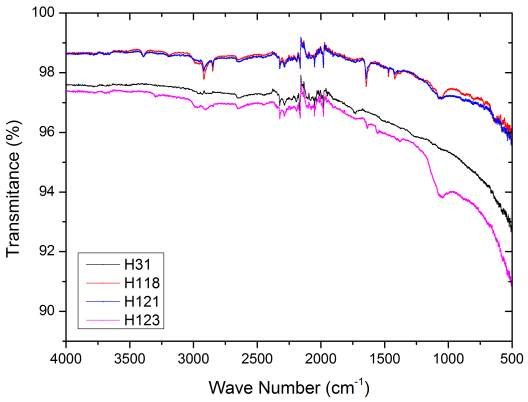

FIG. 9: Transmittance obtained vs the wave number for different SMCs submitted to IR radiation and for pure iron (H31). Both the peaks at 2000 cm^{-1} and the decay at high energies are characteristic of the metallic Fe - Fe bond.

To identify it, we submit the different SMCs to Infrared Radiation (IR). Both the absorption peaks around 2000 cm^{-1} and the soft decay at high energies are the typical behavior of the iron particles, whose metallic bonding is very strong, and it can only be excited by absorbing high energy radiation. But we also see a small absorption peak at 1000 cm^{-1} in each of the SMCs, corresponding to the excitation of a covalent bond, which we identify as a phosphate covering [7].

The H118 shift present a deeper peak, and a more pronounced decay of the transmittance at high energies. H121 and H123, on the other hand, behave in the same way.

The different nature of the phosphate covering, together with the mean size of particles obtained by laser diffraction shown in section I, lead to the variations observed in the behavior of the magnetization and the permeability between the different SMCs.

Acknowledgments

I want to thank both Dr. Javier Tejada and Dr. Arturo Lousa for being my advisors during this project, in which I have learned so much. By working with them I have been able to understand the importance of discipline, constancy and creativity needed for research. I would like to also thank the guidance and support received by doctoral student Jaume Calvo all these months, showing me the most experimental side of physics, which I learned to appreciate more than I ever expected.

Finally, I would like to thank Javier for have taught me the first fundamentals of quantum physics when I first chose the branch of Theoretical Physics, and a deeper subject this year on pure magnetism. Your passion for science has been such an example to me during these years. I have sincerely enjoyed this year, and developed true admiration and respect for both, my work and advisors.

[1] B. Yang, Z. Wu, Z. Zou, and R. Yu, "*High-performance Fe/SiO 2 soft magnetic composites for low-loss and high-power applications*", J. Phys. D. Appl. Phys., vol. 43, no. 36, p. 365003, 2010.

[2] T. H. Kim, K. K. Jee, Y. B. Kim, D. J. Byun, and J. H. Han, "*High-frequency magnetic properties of soft magnetic cores based on nanocrystalline alloy powder prepared by thermal oxidation*", J. Magn. Magn. Mater., vol. 322, no. 16, pp. 24232427, 2010.

[3] Eugene M. Chudnovsky & Javier Tejada "*Lectures on Magnetism*", 1st. ed. (Princeton, New Jersey, 2006), Ch. 1.4 & 3.3.

[4] Toroid (Figure), https://www.allaboutcircuits.com/technical-articles/a-review-of-basic-magnetic-theories/

[5] R. Dosoudil, E. Uk, and V. Olah, "*Computer controlled system for complex permeability measurement in the frequency range of 5 Hz - 1 GHz*", J. Electr. Eng., vol. 57, no. 8 SUPPL, pp. 105109, 2006.

[6] Eugene M. Chudnovsky & Javier Tejada "*Lectures on Magnetism*", 1st. ed. (Princeton, New Jersey, 2006), Ch. 1.5

[7] E.-L. Karjalainen, A. Hardell, and A. Barth, "*Toward a general method to observe the phosphate groups of phosphoenzymes with infrared spectroscopy*", Biophys. J., vol. 91, no. 6, pp. 22829, 2006.